

Contents

1. Things to do	3
1.1. Experiment 1: measurement of the band gap energy	3
1.2. Experiment 2: The Haynes & Shockley-experiment	3
1.3. Experiment 3: semiconductor detectors	3
2. Theoretical Basics	4
2.1. Band model	4
2.2. Characterisation of semiconductors	5
2.2.1. Direct and indirect semiconductors	5
2.2.2. Intrinsic and extrinsic semiconductors	6
2.3. p-n-diode	6
3. Experiment 1: measurement of the band gap energy	8
3.1. Setup	8
3.2. Procedure	9
3.3. Data analysis	9
3.3.1. Silicon	11
3.3.2. Germanium	13
4. Experiment 2: Haynes & Shockley-experiment	15
4.1. Setup	15
4.2. Procedure	15
4.3. Data analysis	15
4.3.1. $U = \text{const}$	15
4.3.2. $d = \text{const}$	19
5. Experiment 3: semiconductor detector	23
5.1. Setup	23
5.2. Procedure	23
5.3. Data analysis	23
6. Summary and discussion	29
A. List of Figures	32
B. List of Tables	32
C. References	33
D. Appendix	34
D.1. Extra plots	34
D.2. Original data	36

1. Things to do

1.1. Experiment 1: measurement of the band gap energy

The goal of this experiment is, to get the band gap energy of silicon and cadmium telluride. The absorption and transmission coefficients, with are needed for the calculation get experimentally detected. In order to get them the following steps must be taken:

- The way of the light shall be optimised with the right optical grid and filter.
- The absorption and transmissions spectrum of the two available samples shall be measured with the software 'LoggerPro'.
- For both spectres a underground measurement is to be taken.
- Errors shall be calculated on the measurement.
- The values of the band gap energy of germanium and silicon shall be calculated, from the transmission and the absorbtion spectra.

1.2. Experiment 2: The Haynes & Shockley-experiment

Now the understanding of the function of a semiconductor shall be deepened:

- The evolution in time and space of a cloud of cavity which has been generated by a laser in an sample of germanium shall be looked at.
- These changes are to be measured: The cavity gets moved by a driver voltage from the laser to a needle which is connected to an oscilloscope. In a first measurement the distance between needle and laser and in a second the driving voltage is changed.
- From the time evolution of the main emphasis of the cavity cloud the mobility μ of free electrons in p-germanium is to be calculated.
- From the change with the time of the strongnes of the signal the average live time τ_e can be calculated.
- From the time evolution of the cavity cloud (standard deviation of a Gauss-plot) the constant of diffusion D_e of a free electron in p-germanium.

1.3. Experiment 3: semiconductor detectors

An application possibility for semiconductors is in the detection of γ -rays. We use for the spectres of two radioactive samples a silicon diode and a CdTe crystal:

- The setup of the detector and its electronic shall be understood.
- The spectres of ^{57}Co and ^{241}Am shall be measured with a silicon diode.
- The spectres of ^{57}Co and ^{241}Am shall be measured with a CdTe crystal.
- With the ratio of the height of the peaks the ratio of the probability for absorption of silicon and CdTe shall be calculated.
- From the position and broadness of the peaks the relative resolution of energy shall be calculated.

2. Theoretical Basics

One can divide materials in three different groups based on their specific resistance. It is defined as

$$\rho = R \frac{A}{l}.$$

Materials with a value of $\rho \leq 10^{-3} \Omega \text{cm}$ are 'normal' conductors. Materials with a specific resistance of $\rho \geq 10^8 \Omega \text{cm}$ are insulators. Semiconductors have values in between those two categories. The specific resistance of semiconductors is heavily dependent on the temperature of the semiconductor.

Semiconductors are mostly made from silicon or germanium. Those are a branch of semiconductors called elemental semiconductors. They are made up of elements from the fourth main group on the periodic table. The other branch is called compound semiconductor, which are a mix of elements from the third and fifth group.

2.1. Band model

Following the laws of quantum mechanics, electrons are forced into certain energy levels while trapped in a potential. Those levels are solutions to the Schrödinger equation.

If an electron is trapped in a potential valley between two atoms, we get discrete energy levels. With two electrons, the stationary wave functions start to overlap. Following the Pauli principle we get two slightly separated energy levels. If we look at a crystal with n atoms and n electrons, instead of discrete levels we get continuous levels which are called bands.

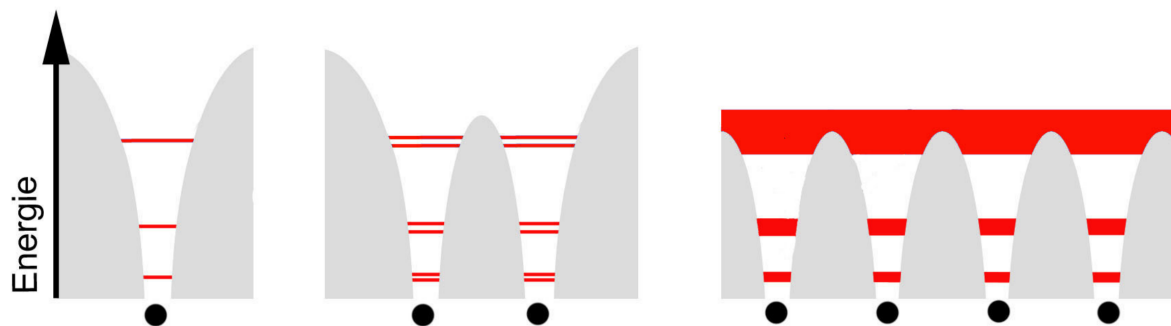


Figure 1: Representation of different energy levels/bands at different amounts of electrons and potential wells.

[Amr, chap. 2.2.1, p.9]

At a temperature of 0 K the bands get filled up, from the bottom to the top till they reach the Fermi edge. The highest, fully occupied band is called the valence band. All fully occupied bands are not conducting, because the sum of the impulses of the electrons is zero. So no electrons move effectively and therefore we have no current density \vec{j} .

If we pump enough energy into the system (e.g. in form of an electro-magnetic-wave or 'light'), some electrons get to move to the band above the valence band, which is called the conducting band. To do so, one electron needs the energy ΔE (E_g) which is the energy width of the bandgap.

While an insulator has a bandgap with an energy difference of many eV, which results in

not electrons getting excited just from thermal stimulation, a semiconductor has an E_g of (depending on the material) 1 eV, which results in thermal stimulation. A normal conductor has no bandgap between the valence and conducting band.

Electrons in the conducting band are called semi-free. They are responsible for the conducting characteristics of a semiconductor. If we have a potential attached to our semiconductor the electrons can move and therefore we can measure a current.

Stimulated electrons leave a hole behind (meaning an then positive charged atom). Those holes can also move, if a potential is attached. But only indirect. The holes recombine with electrons from an neighbour atom, creating a new hole which then recombines with an electron from an neighbour atom and so on.

2.2. Characterisation of semiconductors

2.2.1. Direct and indirect semiconductors

The following illustration shows the energy bands of a silicon and a gallium arsenide semiconductor in the pulse space (Figure 2).

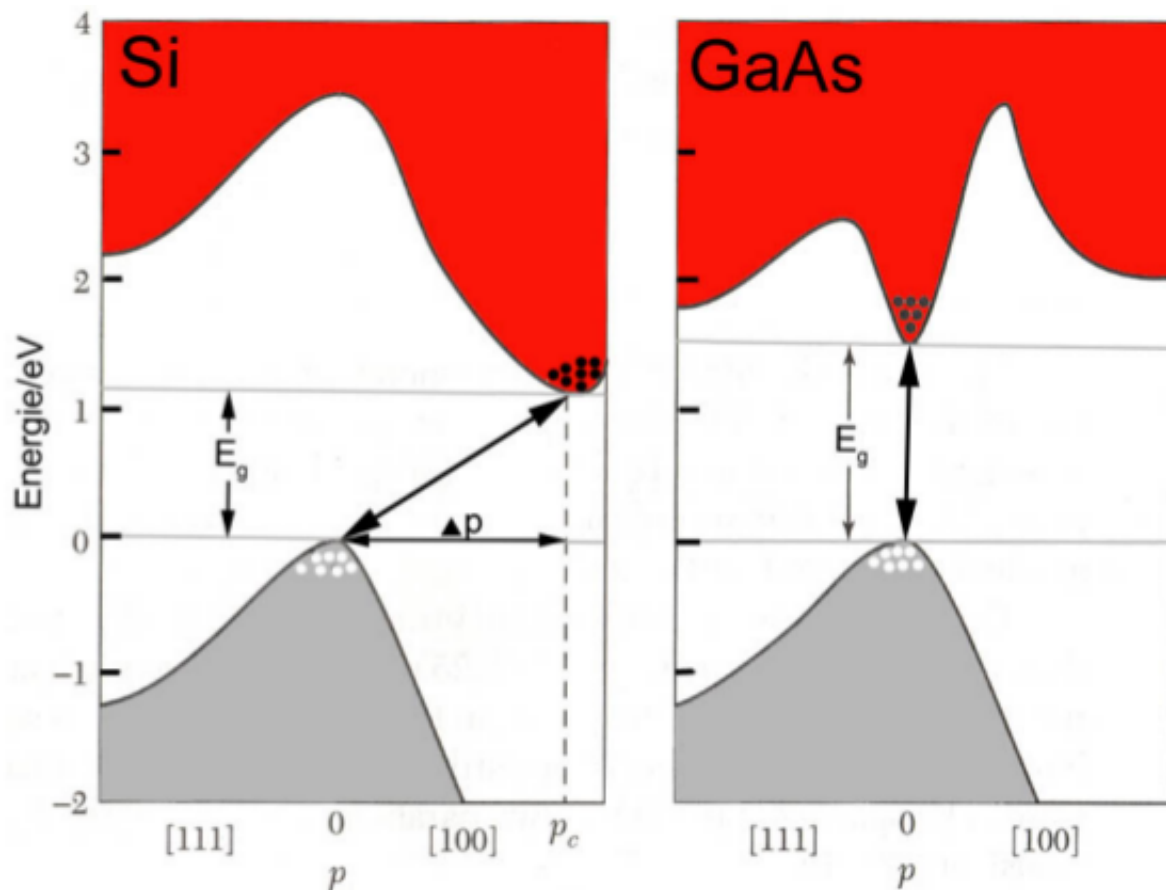


Figure 2: indirect (left) and direct semiconductor (right).
[Amr, chap. 2.4, p.17]

To stimulate electrons we need photons and grid-waves. Grid-waves are described as phonons (quasi-particles). Phonons have high pulse compared to their energy.

Where direct semiconductor only needs energy to overcome the bandgap, the indirect semiconductor also needs pulse. The minimum of the conducting band and the maximum of the valence band of a direct semiconductor are at the same position on the pulse axis of our pulse

space. An example of such conductor is GaAs.

To achieve a direct transmission, the energy of the photon must be greater than the energy of the bandgap E_g :

$$\begin{aligned} E_{\text{photon}} &= \hbar\omega \geq E_g \\ \vec{p}_{\text{photon}} &= \hbar\vec{G} \quad \vec{G} \in \text{reciprocal grid.} \end{aligned}$$

The maximum of the valence band of an indirect semiconductor is shifted sideways to the minimum of the conducting band (Δp). At indirect transitions the pulse of the photon must be connected to the energy of the bandgap via

$$|\vec{p}| = \frac{E}{c}.$$

Because of the Δp a phonon must be present at the transmission. It can be annihilated or created.

For the first case we would have

$$\begin{aligned} E_{\text{photon}} + E_{\text{phonon}} &= E_g \\ \vec{p}_{\text{photon}} + \vec{p}_{\text{phonon}} &= \Delta\vec{p} + \vec{G}. \end{aligned}$$

And for the second

$$\begin{aligned} E_{\text{photon}} &= E_{\text{phonon}} + E_g \\ \vec{p}_{\text{photon}} &= \vec{p}_{\text{phonon}} + \vec{G}. \end{aligned}$$

2.2.2. Intrinsic and extrinsic semiconductors

Intrinsic semiconductors are perfect semiconductors. They have no imperfections in their grid or impurities with foreign atoms. Sadly it is not possible to create such perfect semiconductor. Intrinsic semiconductors are only theoretical ones. Real ones are called extrinsic. They have imperfections in their grid and or impurities. Those imperfections and impurities can result in some strange and unwanted energy levels, which result in different conducting characteristics. An atom from an intrinsic semiconductor would have four valence bonds. In an extrinsic, we could have a foreign atom which has for example five or three valence bonds. With only three bonds, there would be a hole, because an electron is missing. With five valence electrons we would have an extra semi-free electron. Both cases would alter our conducting characteristics. Most impurities are unwanted. Wanted ones are called doping.

2.3. p-n-diode

A p-n-diode is a n-semiconductor (i.e. it has surplus electrons) that joins a p-semiconductor (i.e. it has surplus holes). Because of the surplus of electrons and holes in each layer it results in the electrons and holes moving to the joined area and annihilating each other. That zone is called barrier layer and is $1\mu\text{m}$ to $10\mu\text{m}$ thick. The ionised atom layers form an electrical field, which suppresses more diffusion/movement of holes and electrons from each layer to one another. In Figure 3 the equilibrium distribution of the charge carrier densities are shown.

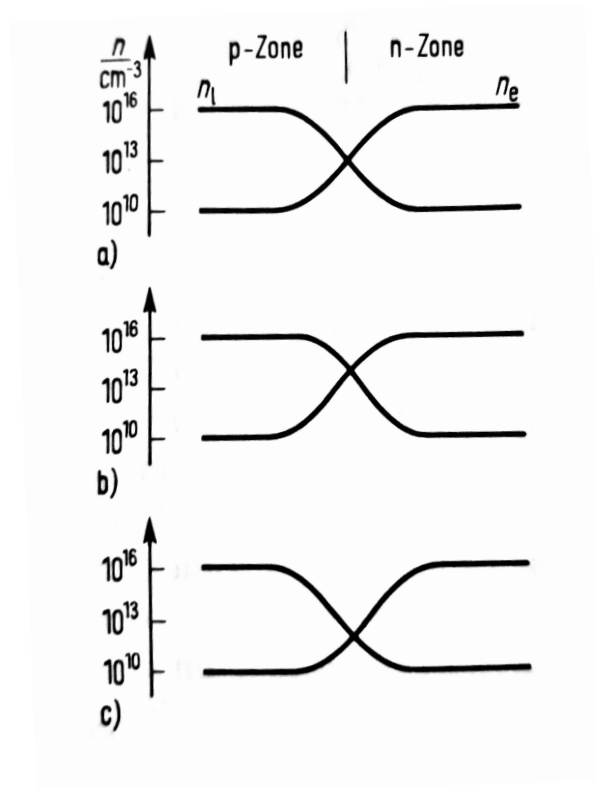


Figure 3: electron-density n_e and hole-density n_i at a p-n-crossing.
 [Wal, chap. 5, p.280]

We can see that the number of electrons and holes are rising in the barrier layer (in the middle/b), if a current flow is poled in the passage direction (meaning that the positive pole is connected to the p-zone). If the current flow is poled against the passage direction (blocking direction) the number of electrons and holes are sinking again (c).

3. Experiment 1: measurement of the band gap energy

3.1. Setup

The schematic setup in figure 4 shows the way of the light. The angle between both arms of the optical bank is 15° . We use light of a lamp, that gets put in a straight bundle with the help

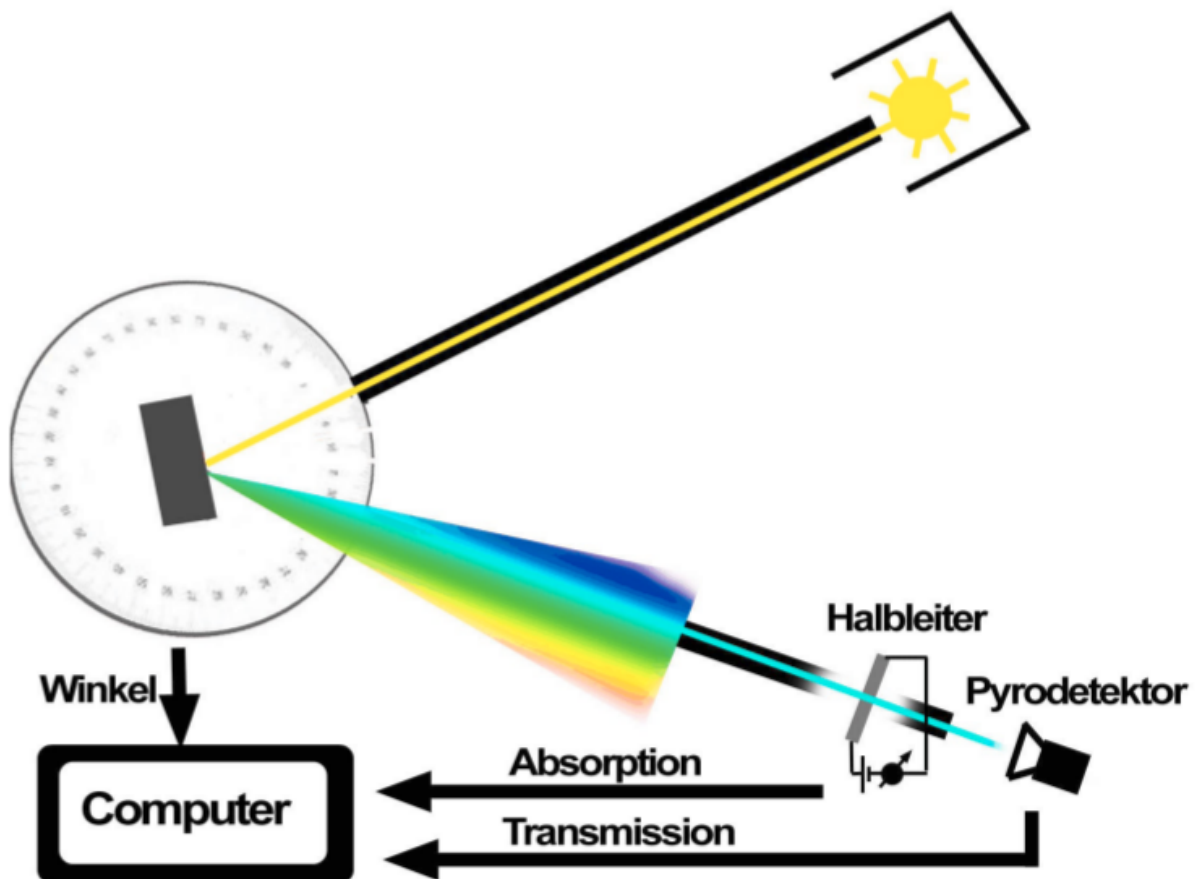


Figure 4: Schematic setup, measurement of the band gap.
[VeFP, chap. 2.4, p.4]

of a lens. Directly behind the lamp there is a so called chopper. This pulses the light with a frequency of about 70Hz. Thanks to this the noise of the measured data can be reduced with a Lock-In amplifier. The beam of light hits an optical grid. The grid can be turned. With the help of the formula

$$E(\phi) = \frac{hc}{2d \sin(\phi) \cos(\psi)}$$

ϕ : angle of the optical grid,

h : Planck-constant,

c : speed of light,

d : gridconstant,

ψ : half opening angle of the bank = $7,5^\circ$

the computer calculates the energy of the light in a specific angle. From here the spectrum comes to the sample (first silicon and in the next part germanium), again focused by a lens and an aperture with a width of about 2 cm. In order to measure the absorption of the sample, we

measure the electric resistance. The transmission is detected by a pyrodetector. In to measure better spectra, there are special filters, which can be built onto the optical bank.

3.2. Procedure

At first we tried to get the the beam of light as straight as possible on the grid. Since we wanted to measure silicon, we put 0.75 mA on the U-I-changer. On the motor, that moves the grid, we put the grid, which is optimised for silicon. On the computer we then had to set some values. After this we then moved the grid from around -70 to 70 degrees in order to get the data. With this setup we then measured:

- The absorption- and the transmission spectrum
- The background by covering up the sample
- The radiation power of the lamp (without a sample)

These measurements we then repeated for germanium. Here we had to change the U-I-changer to 15 mA.

3.3. Data analysis

The evaluation of the measured data was done with Python. In the following some plots don't have error bars. That's due to the fact that they are either too small to be visible or they were intentionally omitted for the sake of clarity.

We calculate the errors of the absorptions and transmissions by measuring the intensity of the light crossing and being absorbed by the sample thirteen times near the first bending maximum. Of these we calculate the mean value. The errors are calculated with

$$s_{\bar{x}} = \frac{1}{\sqrt{n}} \sqrt{\frac{1}{n-1} \sum_i (x_i - \bar{x})^2}.$$

The results are shown in Table 1.

	transmission	absorption
silicon	$3.233 \cdot 10^{-16} \text{ V}$	0 V
germanium	$1.599 \cdot 10^{-16} \text{ V}$	$2.388 \cdot 10^{-16} \text{ V}$

Table 1: errors on amplitudes

We assume, that the reason, why we get no error for the absorption in the silicon, results from a plug, which didn't hold properly in the pin.

The method we use for the data analysis to get the band gap energies of silicon and germanium is shown in Figure 5.

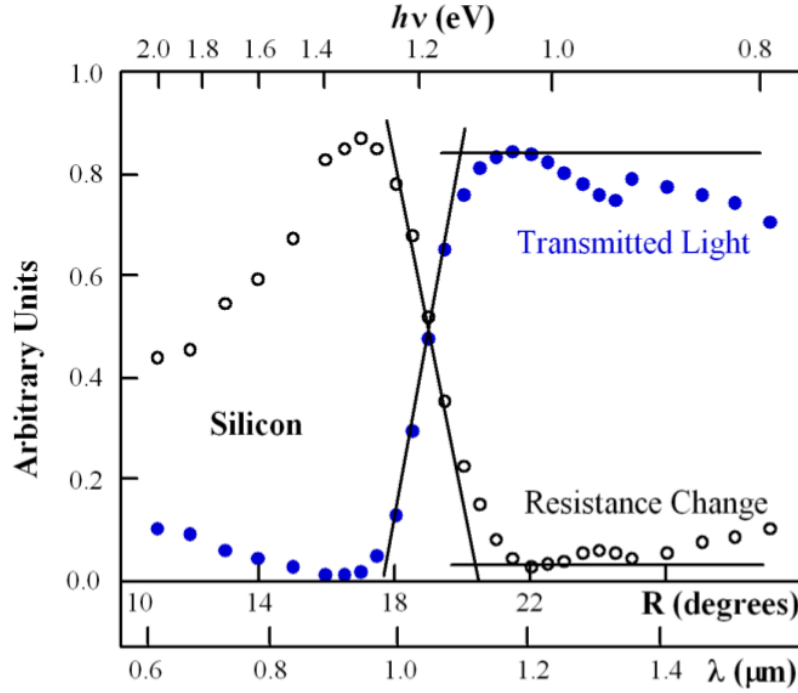


Figure 5: Method of the analysis.
[VeFP, chap. 2.5, p.5]

At first we subtract the signals from their background and scale it on the power of the lamp:

$$Trans_{real} = \frac{Trans - Untergr_{Trans}}{Lampe} \quad Absorp_{real} = \frac{Absorp - Untergr_{Trans}}{Lampe}. \quad (3.1)$$

Then we plotted, using Equation 3.1 the manipulated intensities of the transmitted and the absorbed light over the wavelength. Because we are only interested in special areas, in which there are characteristic intersections between the transmission and absorption plot, only these areas are shown in the following. These areas are at the first diffraction maximum. We fitted linear functions to the measured data left and right of these transmissions. The intersection point of these fits gives the wavelength of the photons with the energy we are looking for. The horizontal lines are fitted to the maximum of the transmission and the minimum of the absorption spectrum. They give borders in which it is possible to get electron-hole pairs.

In order to get the error of the energy we have to calculate at first the error of the wavelength. We do this by using the linear approximation:

$$s_{\lambda} = n \cdot \frac{s_a}{a}$$

where n is the number of measurement points used for the linear fit, a is the slope of the fit and s_a its error. From this we get with Gaussian error propagation an error for the energy. Furthermore there is a systematic error which takes into account, that we always have not one specific energy, but a bundle of different energies on the sample (see Figure 6).

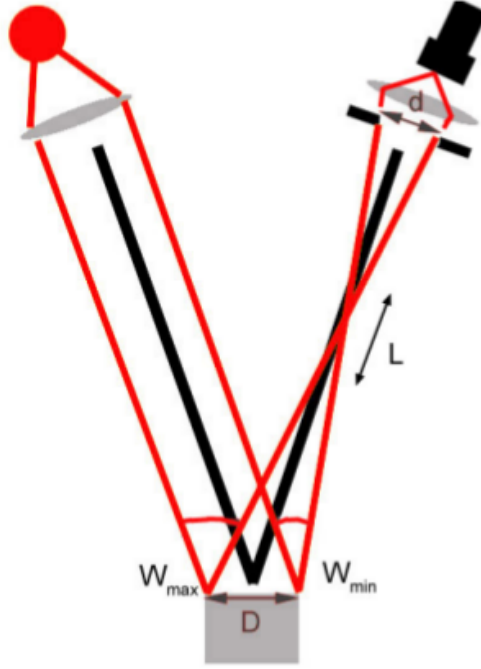


Figure 6: Way of the light.
[Amr, ,chap. 3.4,p.41]

For this we used the following formulas (from [Amr, ,chap.3.4, p.41]):

$$W_{min}(\Phi) = \Psi + \arcsin\left(\frac{\sin(\Psi)L - D/2 \cos(\Phi) - d/2 \cos(\Psi)}{L}\right)$$

$$W_{max}(\Phi) = \Psi + \arcsin\left(\frac{\sin(\Psi)L + D/2 \cos(\Phi) + d/2 \cos(\Psi)}{L}\right)$$

$$s_{E_{syst}} = \frac{1}{2} \left(\frac{hc}{2d \cos(\Psi) \sin(W_{min}/2)} - \frac{hc}{2d \cos(\Psi) \sin(W_{max}/2)} \right)$$

Here L is the distance between the optical grid and the lens, d is the width of the aperture, $D=2.5$ cm is the broadness of the grid and Ψ is half the angle between the arms of the optical bank.

The two errors are added by

$$s_E = \sqrt{s_{E_\lambda}^2 + s_{E_{syst}}^2}.$$

3.3.1. Silicon

Figure 7 shows the spectrum and the linear fit of the bending maximum at the negative angle. Figure 8 shows the same for the positive angle. The whole measured data can be found in the appendix in Figure 27. In Table 2 and 3 are the important data of the linear recursions and the value of the x-axis of the intersection, which gives us a wavelength. In the plots of our data analysis we connected the measurement data with lines in order to increase the clarity.

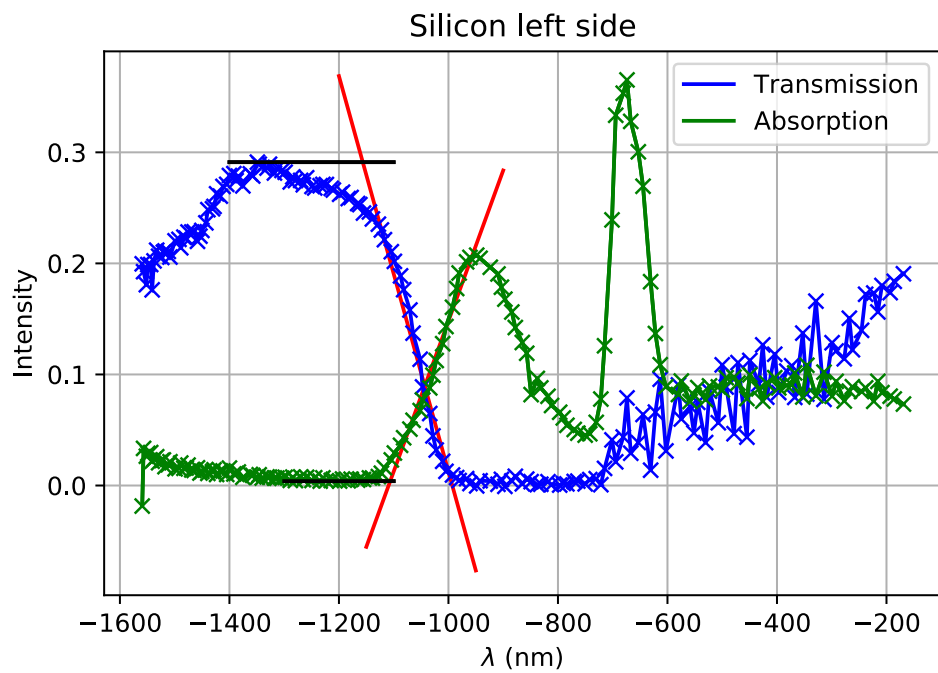


Figure 7: Calculation of the wave length for silicon at negative angles.

Regression for transmission	$-0.0018x - 1.8$
Regression for absorption	$0.00136x + 1.50$
Wavelength	$(1043 \pm 205) \text{ nm}$

Table 2: data of Figure 7

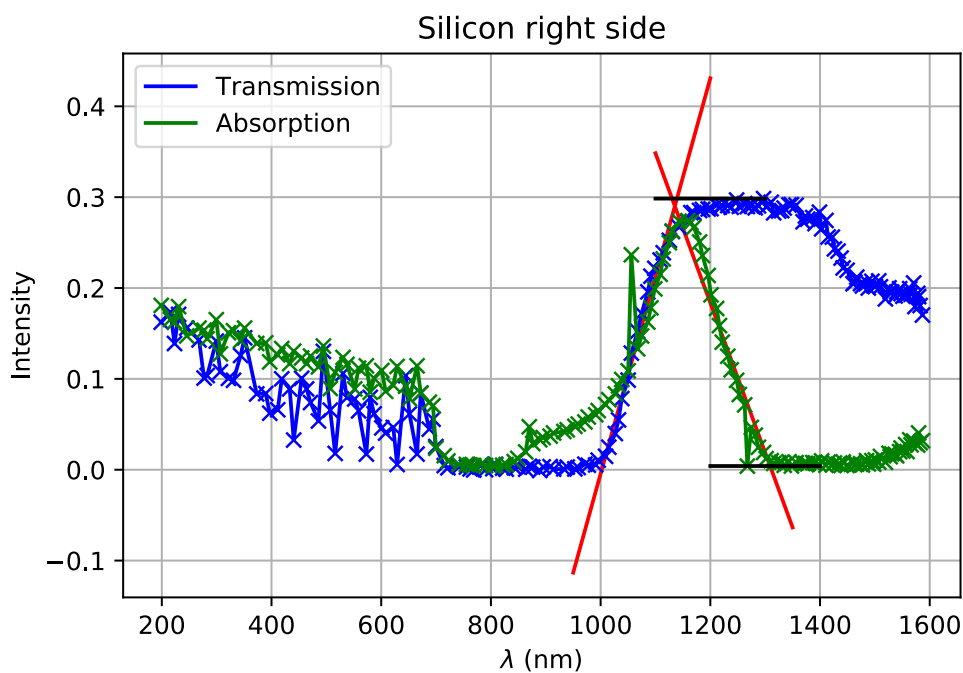


Figure 8: Calculation of the wave length for silicon at positive angles.

Regression for transmission	$0.00218x - 2.18$
Regression for absorption	$-0.0016x + 2.2$
Wavelength	(1135 ± 248) nm

Table 3: data of Figure 8

By taking the weighted middle of the wavelength at the intersection left and right we get

$$\lambda = (1080 \pm 158) \text{ nm}$$

for the wavelength of silicon. Form this we calculated with the formulas

$$E = \frac{hc}{\lambda}$$

$$s_E = E \frac{s_\lambda}{\lambda}$$

the band gap energy of silicon. The resulting energy is

$$E_g = (1.1 \pm 0.2) \text{ eV.}$$

3.3.2. Germanium

For the sample of germanium we do the same calculations as with silicon. The results can be seen in Figure 9 with Table 4 and Figure 10 with Table 5 and all of the data we measured in the appendix in Figure 28.

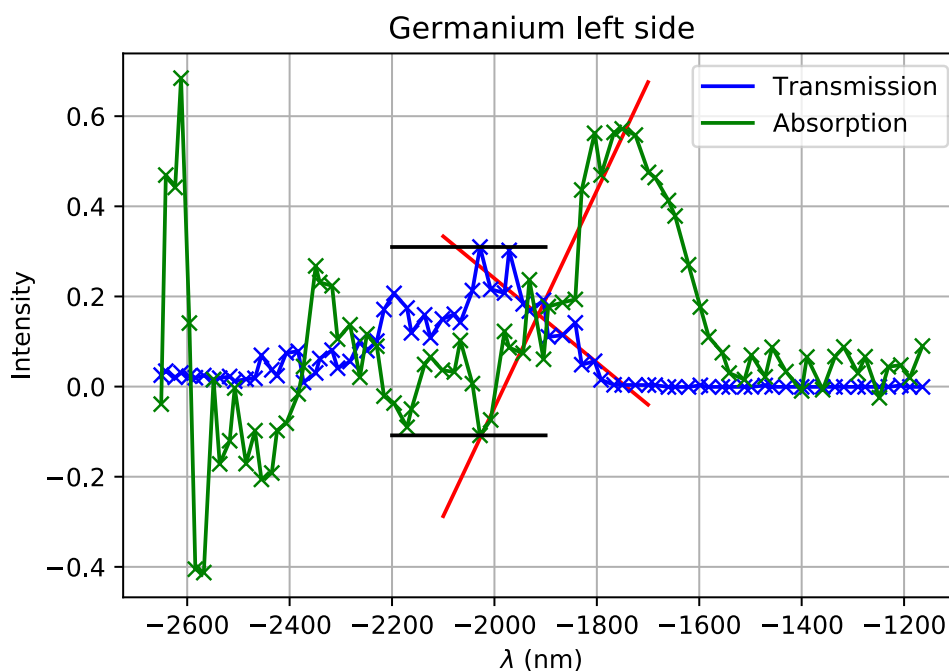


Figure 9: Calculation of the wave length for germanium at negative angles.

Regression for transmission	$-0.00093x - 1.6$
Regression for absorption	$0.0024x + 5$
Wavelength	(1900 ± 30) nm

Table 4: data of Figure 9

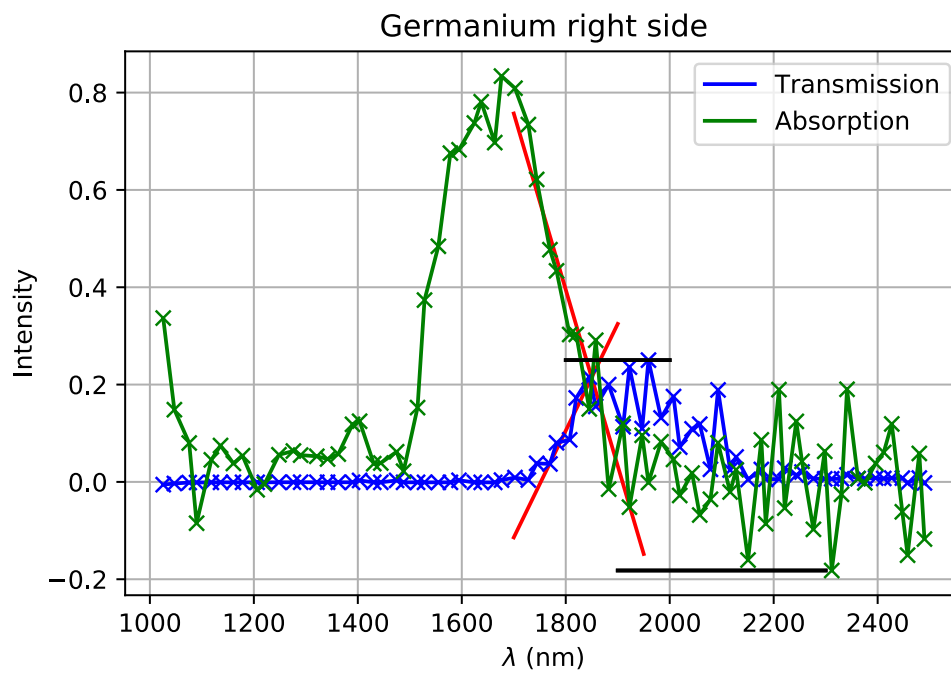


Figure 10: Calculation of the wave length for germanium at positive angles.

Regression for transmission	$0.0022x - 4$
Regression for absorption	$-0.0036x + 6.9$
Wavelength	$(1849 \pm 11) \text{ nm}$

Table 5: data of Figure 10

This time we got a wave length of

$$\lambda = (1874 \pm 21) \text{ nm},$$

and a band gap energy of

$$E_g = (0.661 \pm 0.008) \text{ eV}.$$

4. Experiment 2: Haynes & Shockley-experiment

This experiment is similar to a setup of J. R. Haynes and W. Shockley. They were the first ones who could show the movement of charge in semiconductors.

4.1. Setup

In this experiment a laser, an optical fibre, an oscilloscope and a p-doped sample of germanium are used. The optical fibre leads a laser pulse on the surface of the sample. The energy of the laser pulse must be bigger than the band gap energy. In this way the electrons in the germanium can be brought into the conducting band. On the sample there is a so called driving current. It isn't constant, in order to prevent a over-heating of the sample, so that the germanium can cool down 98% of the time. To improve the result, we can change the intensity of the laser and the point, at which the measurement starts, can be delayed. The driving current can be subtracted of the data with the 'Shifted Output'. With the help of a needle on top of the block, the charge carrier can be detected on an oscilloscope.

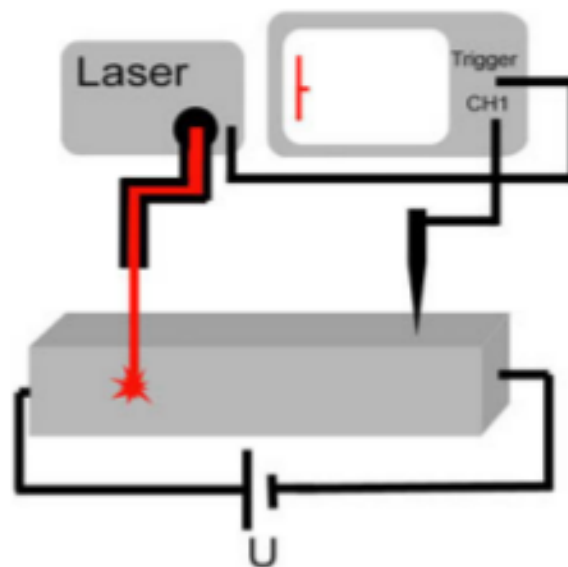


Figure 11: Schematic setup of the Haynes & Shockley-experiment.
[VeFP, chap. 4.2.2, p.47]

4.2. Procedure

After learning, how to use the measuring stick and the oscilloscope, we put a fixed distance of 4.1 mm between the fibre and the needle. Then we varied the driving current between 50 and 25 V in order to get the characteristic Gauss-function on the oscilloscope. After that we measured with different distances (between 2 and 10 mm) and a fixed voltage.

4.3. Data analysis

4.3.1. $U = \text{const}$

First the collected data from the oscilloscope was plotted (Figure 12). Then we fitted Gaussians to each peak (with d as the distance from the laser to the needle).

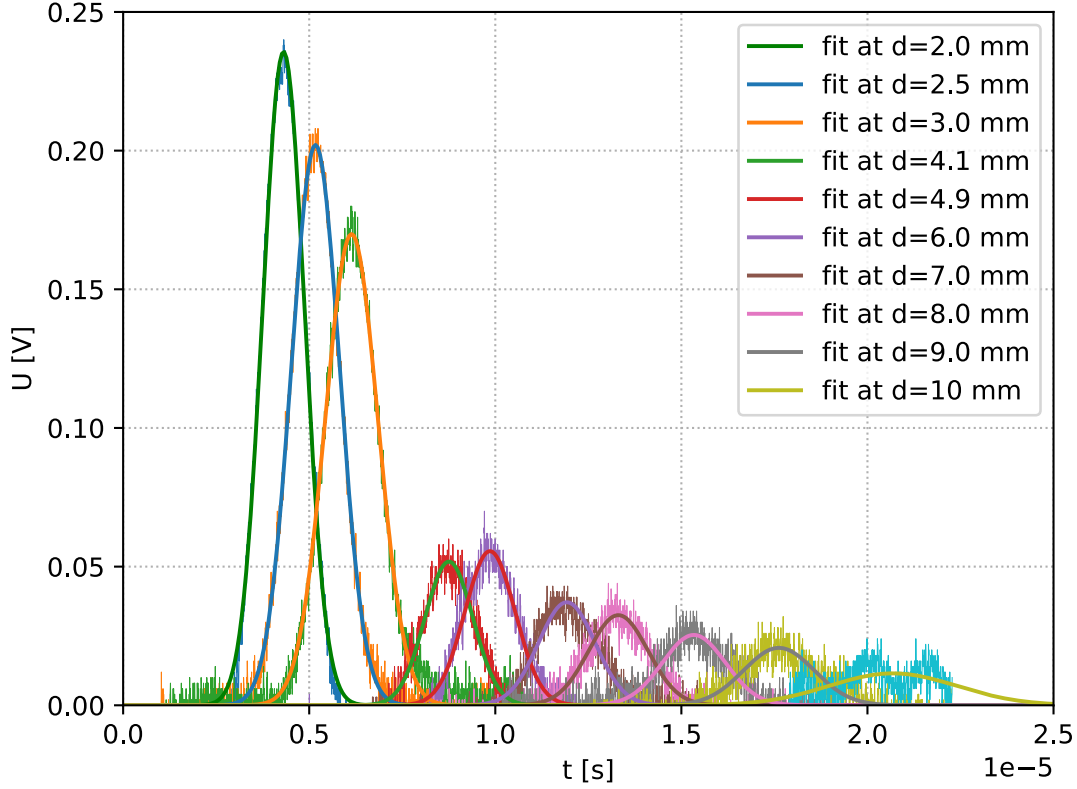


Figure 12: Data and Gaussian fits for the electron clouds at different laser to needle distances.

We can see that the peak at $2 \cdot 10^{-5}$ s is hardly a Gaussian and more of a m-shaped distribution. Therefore the fit data for that peak is left out in most of the following calculations. While the amplitude and position gave reasonable data, the variance doesn't make any sense in the context of the other data and the theoretical background behind the experiment.

By comparing the Gaussian

$$\text{Gauss} = A \cdot \exp\left(-\frac{1}{2} \left(\frac{x - x_{\text{center}}}{\sigma}\right)^2\right)$$

to the solution of the differential equation, which describes the movement of the electron clouds

$$c(t, x) = C \cdot \exp\left(-\frac{t}{\tau_n}\right) \cdot \exp\left(-\frac{(x - \mu_n Et)^2}{4D_n t}\right),$$

with μ_n as the mobility of the electron cloud, τ_n as the mean lifetime of a cloud and D_n as the diffusion constant, we can derive

$$x_{\text{center}}(t) = \mu_n Et \quad A(t) = C \cdot \exp\left(-\frac{t}{\tau_n}\right) \quad \sigma(t) = \sqrt{2D_n t}. \quad (4.1)$$

Therefore we have to do 3 different fits. First we start with the amplitude.

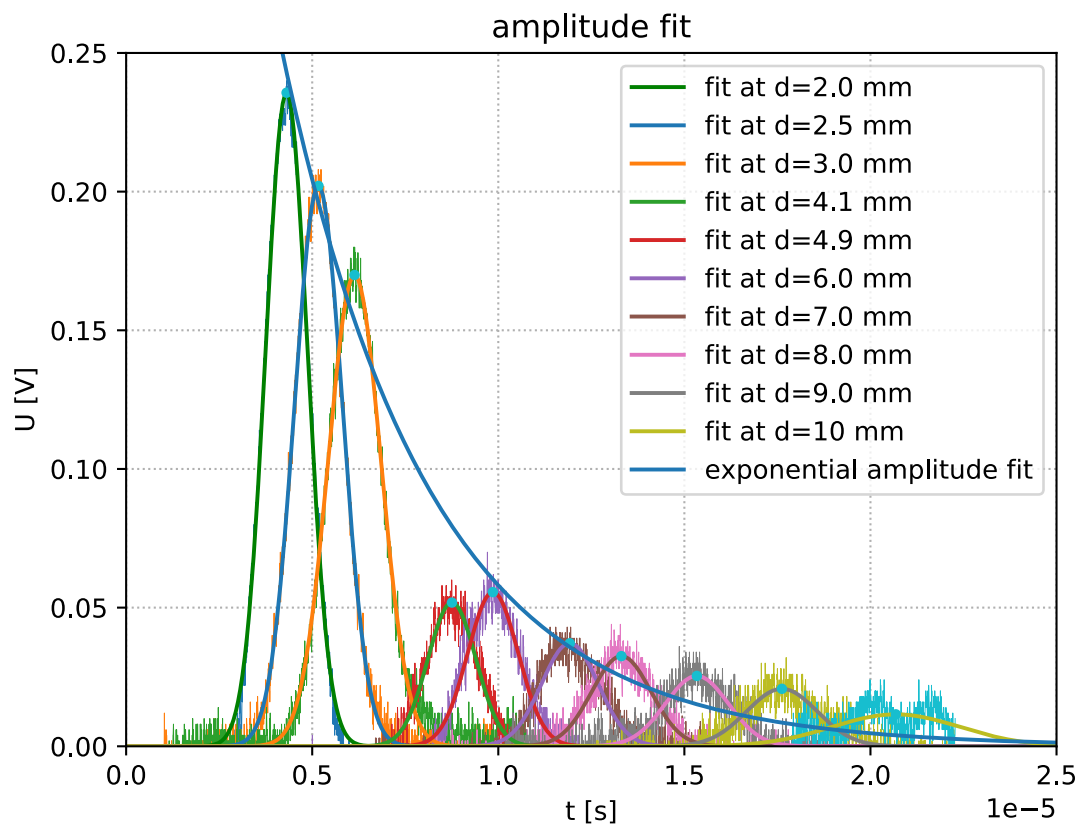


Figure 13: Exponential fit of the amplitudes of our Gaussian fits.

τ_U is one of our fit parameters and is equal to

$$\tau_U = (3.8 \pm 0.4) \mu\text{s}.$$

Next we calculated the velocity of the electron clouds. We would expect a linear curve, meaning that the distance of the laser and the needle doesn't influence the speed of the electrons. To do so, we plotted the distance of the laser to the needle, against the time it took the amplitudes from the clouds to reach the oscilloscope. Then we did a linear fit.

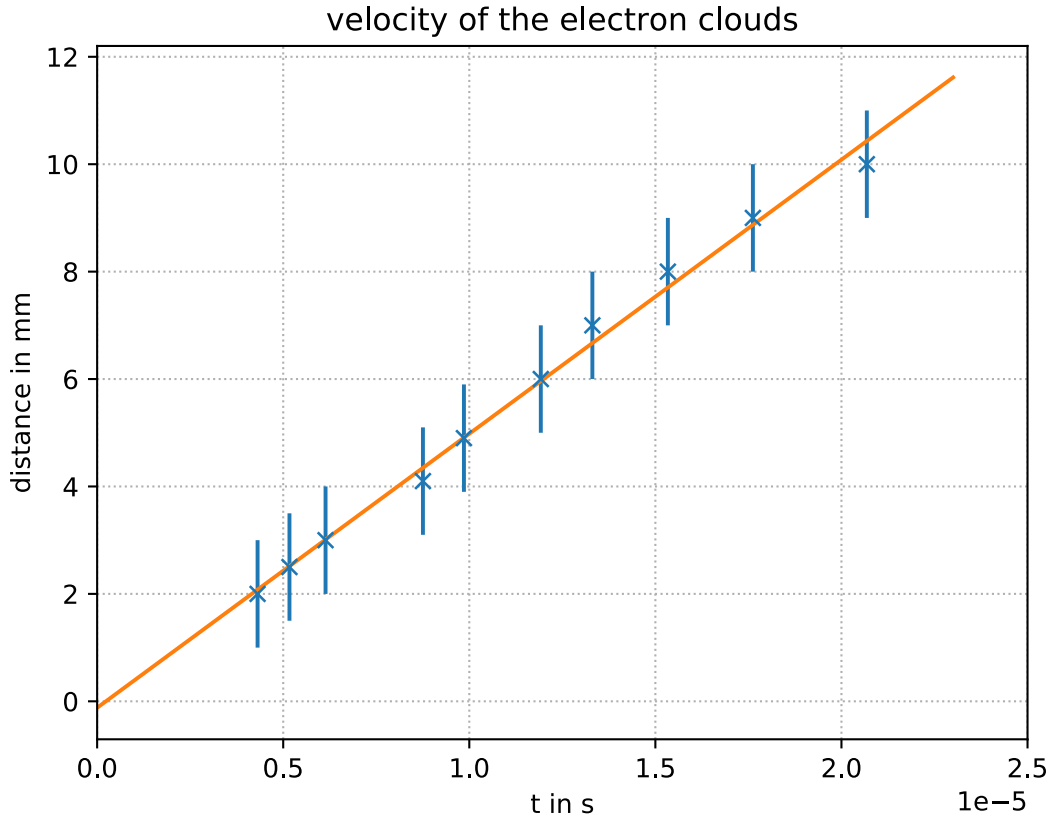


Figure 14: Velocity of the electron clouds with a linear fit.

We can see, that it is indeed linear. Therefore the clouds have all the same velocity and we can get the value of the velocity from our fit parameter

$$v_U = (510 \pm 15) \frac{\text{m}}{\text{s}}.$$

The electrons move at roughly $0.0000017c$. Therefore we don't have to use relativistic equations and can operate with classical physics.

With the applied voltage $U = (50 \pm 2) \text{V}$ and a length of $l = (30.0 \pm 0.1) \text{mm}$ for our germanium block we get a electric field strength of

$$E_U = \frac{U}{l} = (16.7 \pm 0.9) \frac{\text{V}}{\text{cm}}.^\dagger$$

The mobility μ_U can now be calculated via

$$\mu_U = \frac{v}{E} = (3061 \pm 182) \frac{\text{cm}^2}{\text{Vs}}.^\dagger\dagger$$

Last but not least, we calculated the diffusion constant D_n using $\sigma(t) = \sqrt{2D_n t}$.

Because we weren't able to get a proper fit for the square root function we plotted the squared function. Then we fitted it linearly.

[†] $s_{E_U} = E_U \cdot \sqrt{((s_U/U)^2 + (s_l/l)^2)}$

^{††} $\mu_U = \mu_U \cdot \sqrt{(s_v/v)^2 + (s_E/E)^2}$

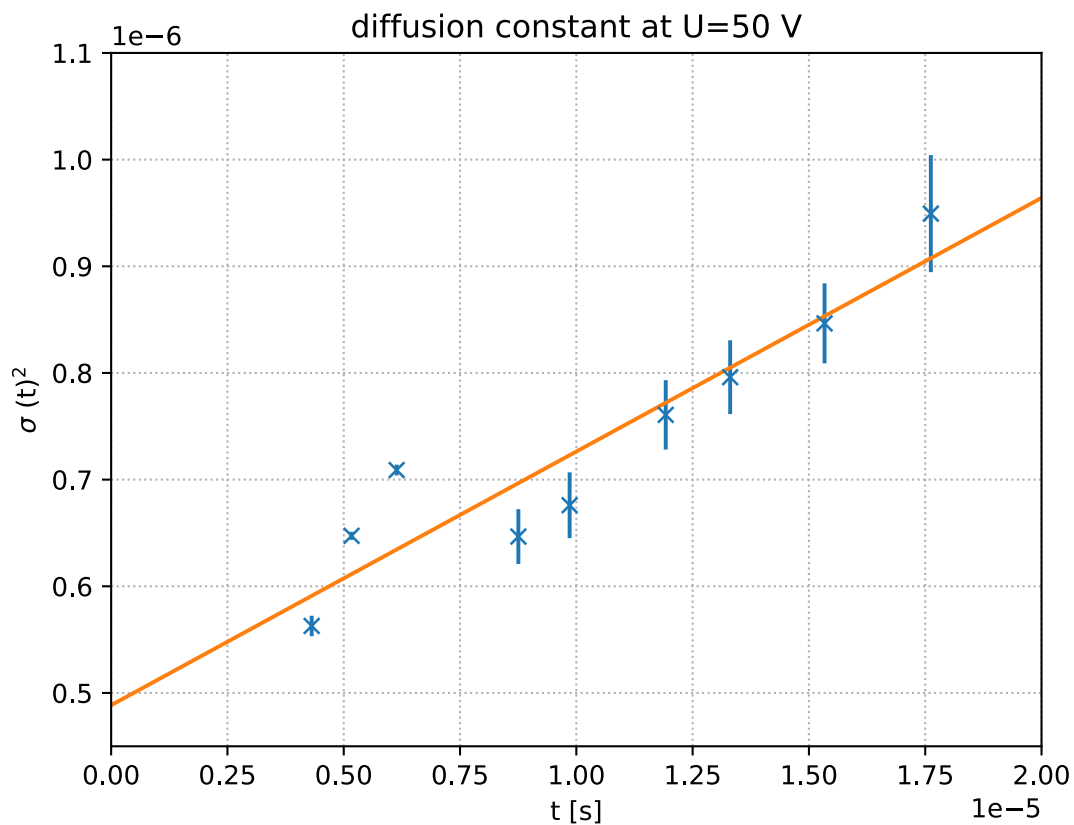


Figure 15: Plot and linear fit for the squared diffusion constant.

The diffusion constant is now one half times of the square root of the fit parameter. As we can see in Figure 15 the first three points are not on the line and have little error bars. This results in a higher error for our diffusion constant. We get

$$D_U = (154 \pm 29) \frac{\text{cm}^2}{\text{s}}.$$

4.3.2. $d = \text{const}$

The next part is more or less analogous to the first part. Now we have instead of a different distance a different voltage applied. First we plotted the collected data.

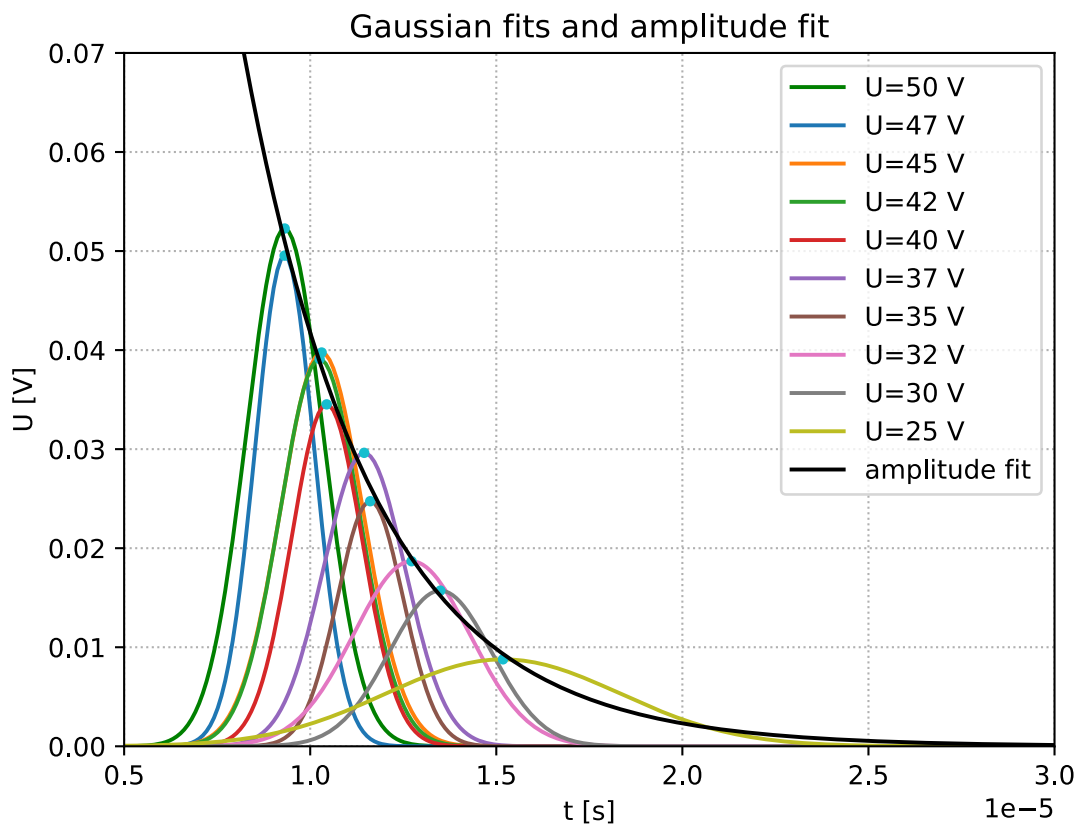


Figure 16: Exponential fit of the amplitudes of our Gaussian fits.

Because of the noisy data, we show only the fits of the peaks. The full plot is displayed in the appendix (Figure 29).

Then we fitted the amplitudes following the amplitude relation from Equation 4.1. The fitted curve is also shown in Figure 16. For the mean lifetime we get

$$\tau_d = (3.5 \pm 0.2) \mu\text{s}.$$

Next we calculated the mobility.

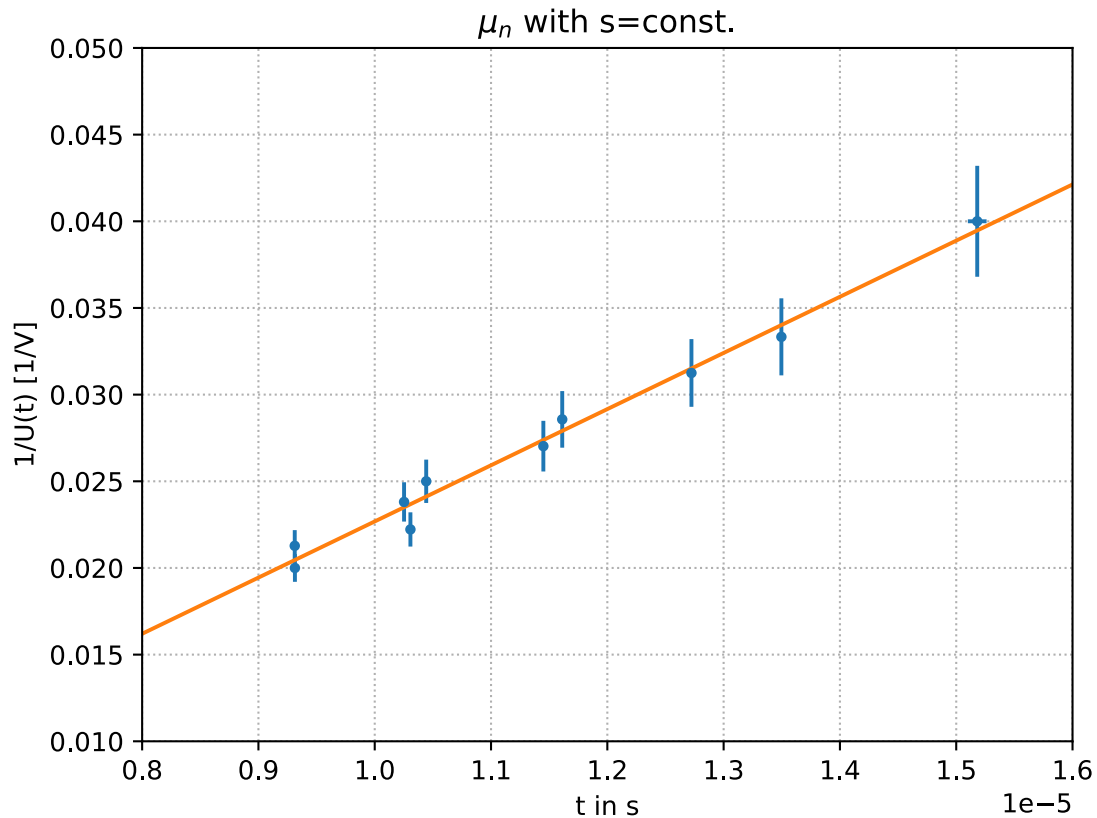


Figure 17: Data and linear fit for the mobility μ_n .

We plotted $1/U(t)$ against t . Then we fitted it linearly and multiplied it with the length l of the germanium block and the distance d from the laser to the needle

$$\mu_d = ld \cdot m,$$

where m is the gradient fit parameter from our linear fit. We get

$$\mu_d = (3985 \pm 141) \frac{\text{cm}^2}{\text{Vs}}.$$

Then we calculated the diffusion constant likewise to the first part.

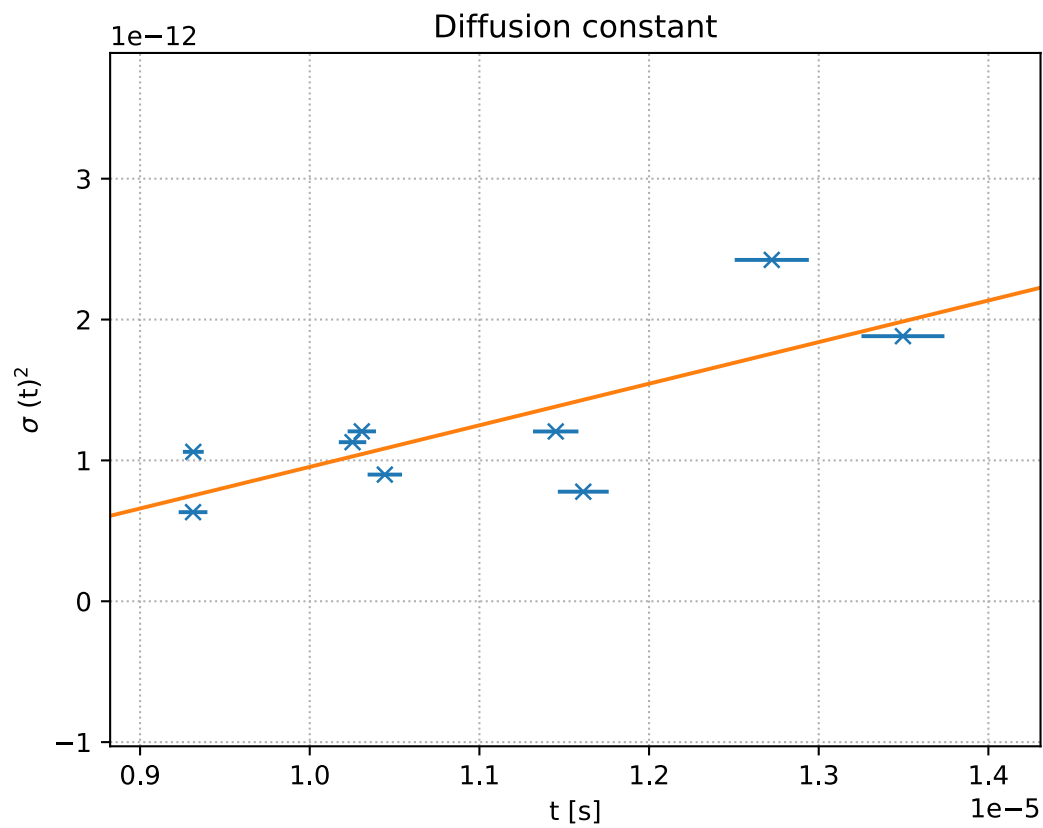


Figure 18: Plot and linear fit for the squared diffusion constant.

The tenth point is not used, because its value for the variance is far greater than for the other peaks (see appendix Figure 30). As a result we get

$$D_d = (108 \pm 31) \frac{\text{cm}^2}{\text{s}}.$$

5. Experiment 3: semiconductor detector

5.1. Setup

The setup is shown schematically in figure 19. As a detector we have a n-n⁺-silicon-diode and a CdTe-crystal. Both are, with their pre-amplifier attached, on exchangeable circuit boards. The pre-amplifier transforms the charge pulses into a voltage. Next the signal goes to the shaping amplifier, which amplifies and optimises the signal to noise ratio. The resulting signal comes to a multi-channel-analyser which sorts the different voltage pulses in different channels, according to their amplitude. They get recorded by the computer.

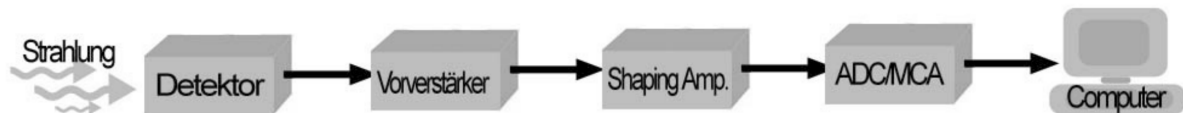


Figure 19: Schematic setup of a semiconductor detector.
[VeFP, chap. 4, p.12]

5.2. Procedure

We measured the radioactive decay of ⁵⁷Co and ²⁴¹Am. For both samples we used both detectors. The measurement time of the experiments with ²⁴¹Am was one hour, that of ⁵⁷Co were two.

5.3. Data analysis

First we plotted the collected data from the experiment (Figure 20 and 22). The error for the y-axis is \sqrt{n} , where n is the number of counts. For the sake of clarity those error bars are not shown here. The plots with error bars are shown in the appendix (see Figure 31 & 32).

Then we fitted a Gaussian-distribution at each peak. The energy for those peaks are known. With the ⁵⁷Co sample in combination with the Si-detector we achieved no significant peak at 136.47 keV. There was one peak, a very small one, which is shown in Figure 24. We fitted it, but that gave us no usable results. Therefore we couldn't calculate the absorption ratio and relative energy-resolution for that energy.

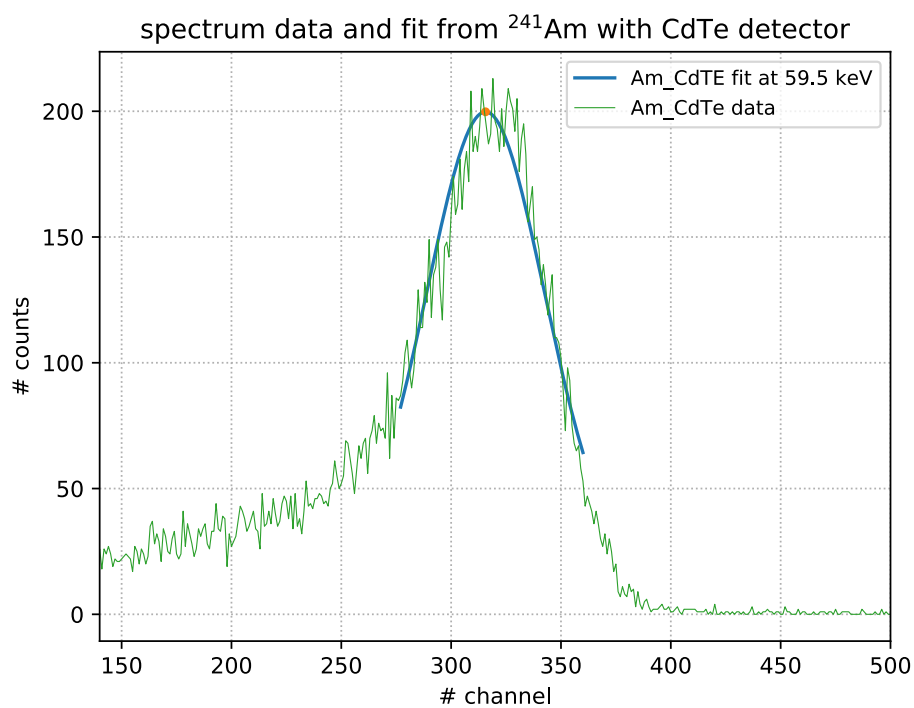


Figure 20: Spectrum from a radioactive ^{241}Am sample using a CdTe-crystal as the detector.

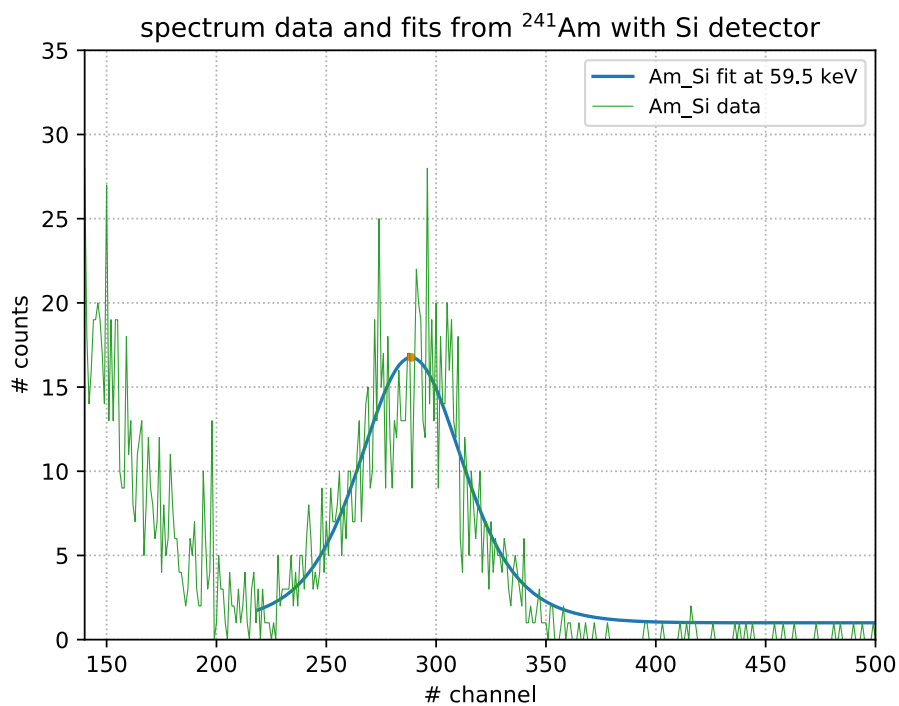


Figure 21: Spectrum from a radioactive ^{241}Am sample using a Si-semiconductor as the detector.

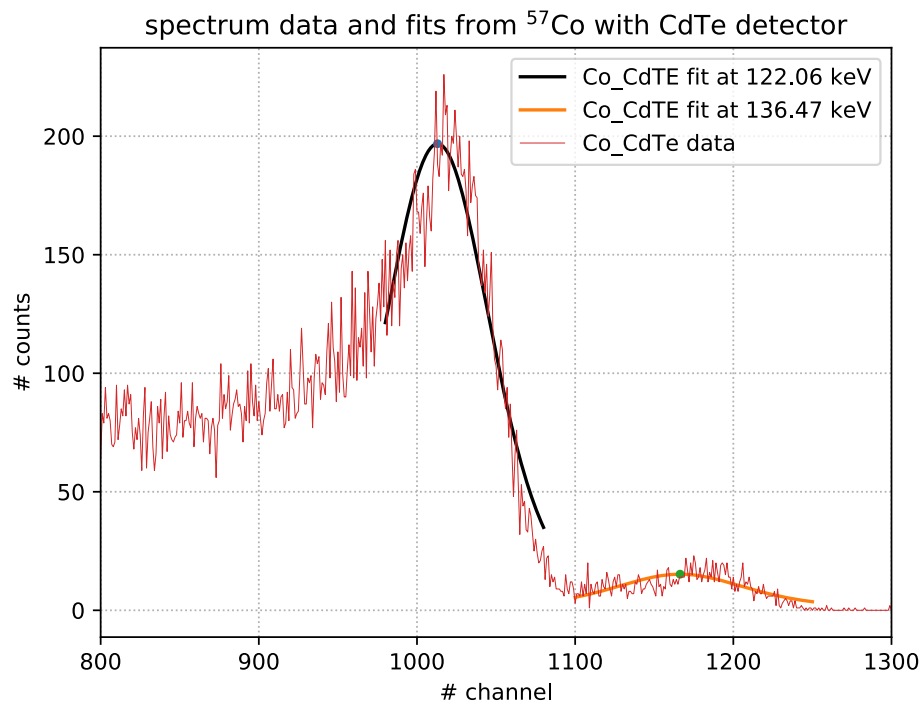


Figure 22: Spectrum from a radioactive ^{57}Co sample using a CdTe-crystal as the detector.

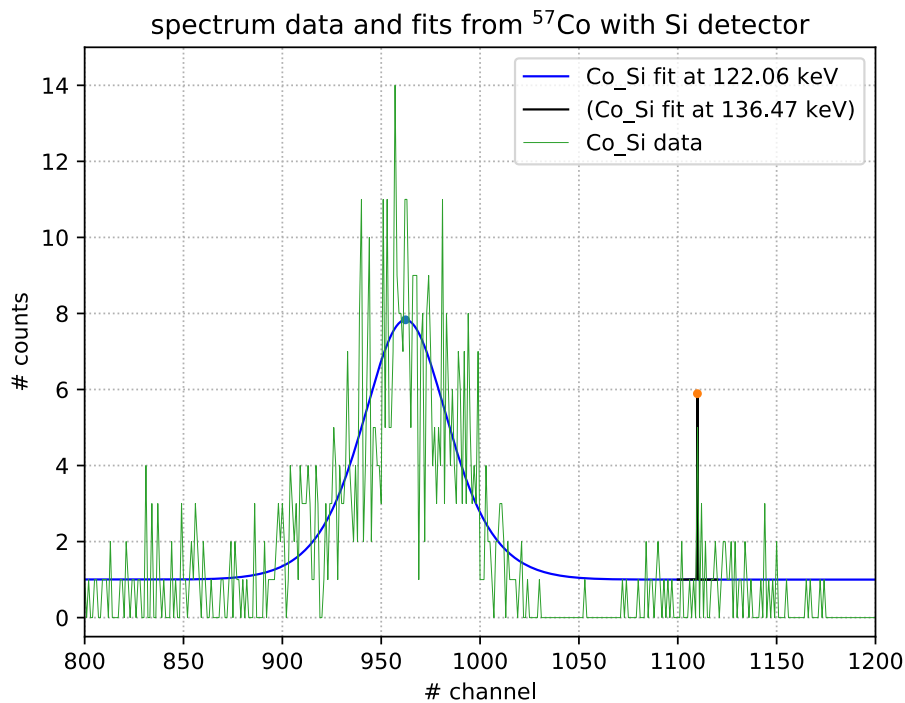


Figure 23: Spectrum from a radioactive ^{57}Co sample using a Si-semiconductor as the detector.

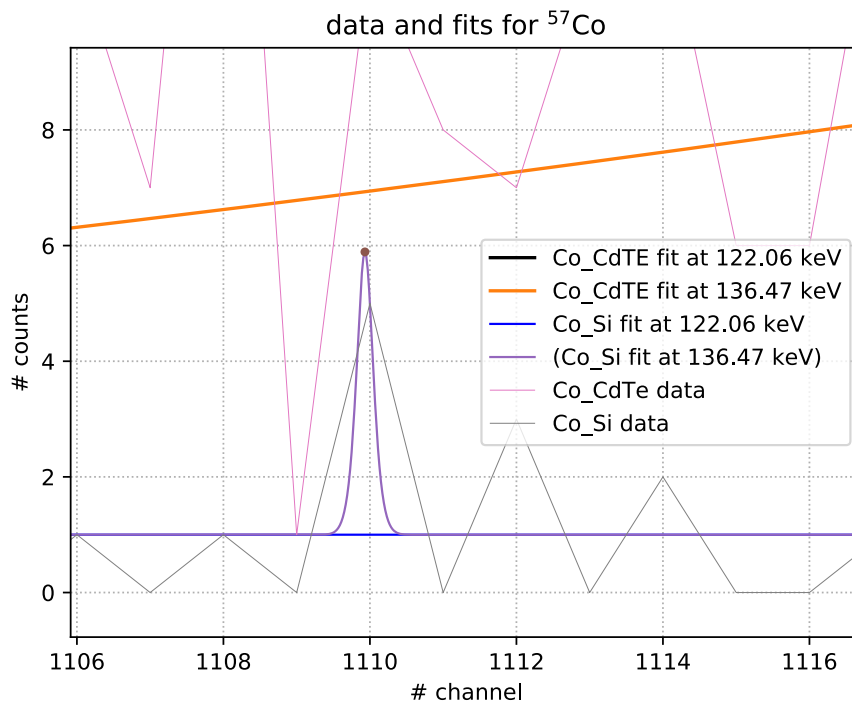


Figure 24: Segment from Figure 23.

With the fits and the known energy values of those peaks we were able to calculate for each detector, what energy corresponds to one channel (Figure 25).

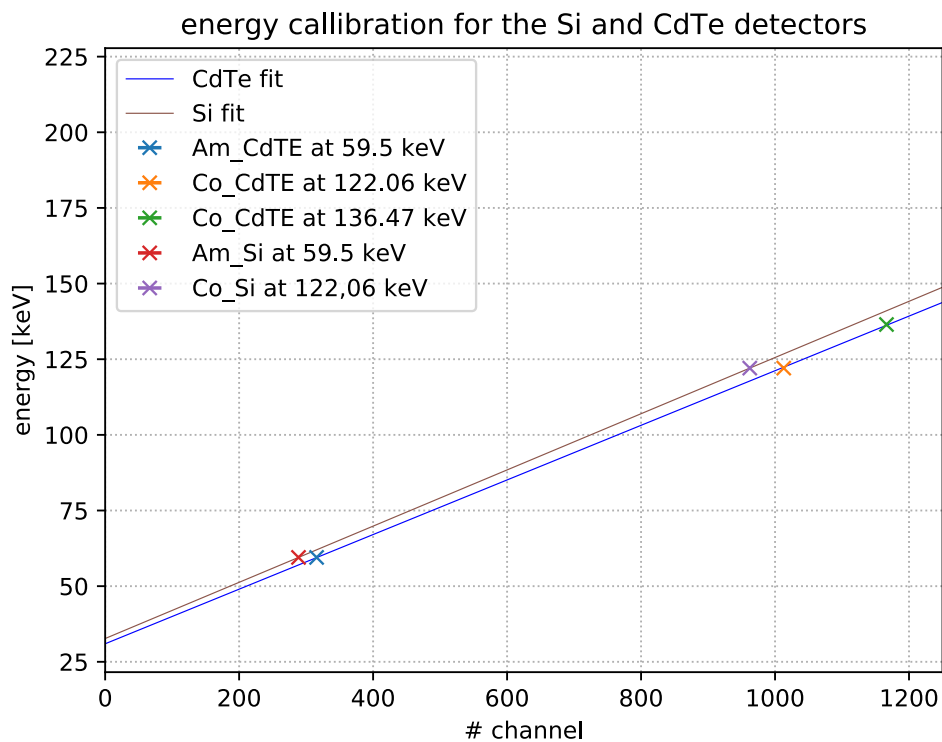


Figure 25: Energy calibration for the Si and CdTe detectors. (The error bars are too small so be visible.)

We can see that the line for the CdTe and Si detectors are close to each other but still different. Therefore we conclude, that different materials have different absorption characteristics. With the energy calibrations we can plot the spectra over the energy (Figure 26). This is only shown for the ^{57}Co probe with the CdTe-detector.

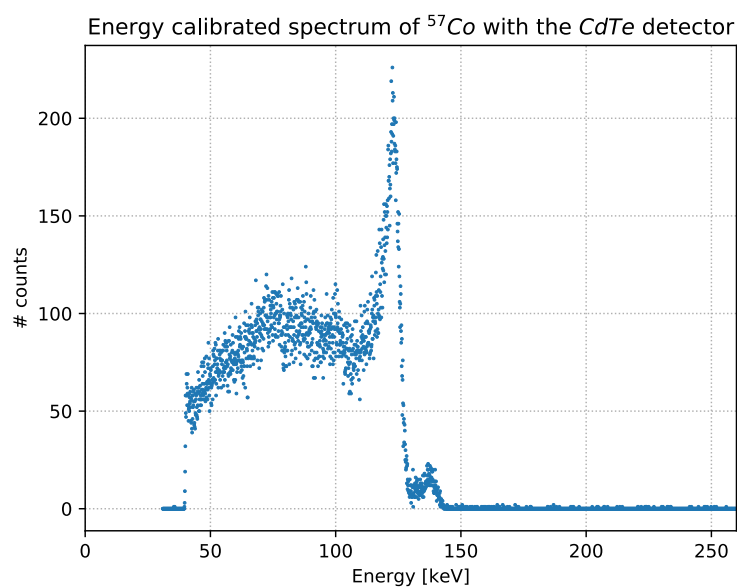


Figure 26: Energy calibrated spectrum of the ^{57}Co probe with the CdTe-detector.

In the next part we actually compare the different absorption probabilities of our two detectors at different energies.

The absorption probability can be derived from the number of counts in one channel over a period of time. In our case it would be the amplitude (A) of our fitted Gaussian. If we compare two measurements, we need to normalise the time for each measurement. We also have to take the effective/active area of each detector into account.

To calculate the ratios we have to follow

$$\frac{Abs_{Si}}{Abs_{CdTe}} = \frac{A_{Si}/a_{Si}}{A_{CdTe}/a_{CdTe}}(E),$$

with $a_{Si} = 100\text{mm}^2$ and $a_{CdTe} = 23\text{mm}^2$ [VeFP, chap. 4.5, p.14, eq.10].

We calculated those ratios for $E = 59.9, 122.06$ and 136.47keV . The errors for the Abs-ratios were calculated using Gaussian error propagation.

peak [keV]	Abs-ratio [%]	Literature [%]
59.5	1.9 ± 0.3	1.40
122.06	1.83 ± 0.07	1.83
136.47	-	2.00

Table 6: Absorption ratios at different energies. [VeFP, chap. 6 ,p.15]

At last we want to examine the relative energy resolution (RER) of each detector at the peak energies.

For doing that we need the full width at half maximum ($FWHM$) instead of the 'normal' standard deviation. Fortunately we can convert the standard deviation of our Gaussians to the $FWHM$ with

$$FWHM(E) = 2\sqrt{2\log(2)}\sigma(E) \approx 2.35\sigma(E).$$

To get the RER we need to divide the $FWHM(E)$ with the energy E . The errors were calculated via Gaussian error propagation.

detector	peak [keV]	RER
Si	59.5	0.318 ± 0.008
	122.06	0.078 ± 0.009
	136.47	-
CdTe	59.5	0.477 ± 0.002
	122.06	0.175 ± 0.004
	136.47	0.139 ± 0.006

Table 7: Relative energy resolution of a CdTe and Si detector.

6. Summary and discussion

The goal of the first part of the experiment was to determine the band gap width of silicon and germanium. In order to achieve this we measured their absorption and transmission spectra. The values we derived from the measurement data are:

- Silicon: $E_g = (1.1 \pm 0.2) \text{ eV}$
- Germanium: $E_g = (0.661 \pm 0.008) \text{ eV}$.

The theoretical values are (from: [VeFP, chap.6, p.15]):

- Silicon: $E_g = 1.12 \text{ eV}$
- Germanium: $E_g = 0.66 \text{ eV}$.

It can be seen, that our values correspond very nicely with the ones from literature.

By comparing it to other literature data (see Table 8) we can see, that it still fits. Although we also see, that the band gap depends on the temperature. But since this temperature dependency is very small and we assume, that we measured near 30 K. Therefore we only have to look at these values which are all very close to our measured data.

	[Kit, chap. 8, p.222]		[Sze, append. G, p.849]	
	0 K	30 K	0 K	30 K
Si	1.17 eV	1.14 eV	1.17 eV	1.12 eV
Ge	0.744 eV	0.67 eV	0.74 eV	0.66 eV

Table 8: Data from the literature.

The fact, that there are different data in literature shows, how difficult it is, to get an exact value for the band gap energy.

The goal of the second experiment was to examine an electron cloud and its properties inside of a germanium block. To do so, we used a laser and an electrical field to produce and move the cloud. We then watched the charge of the electron cloud on an oscilloscope and varied the applied voltage and therefore the electrical field. In the second part we varied the distance between the laser and the needle.

The properties we wanted to measure are the mean lifetime τ , the mobility μ and the diffusion constant D . The values we measured are

	$U = \text{const.}$	$d = \text{const.}$	literature
τ [μs]	3.8 ± 0.4	3.5 ± 0.2	45 ± 2
μ [$\text{cm}^2/(\text{Vs})$]	3061 ± 182	3985 ± 141	3900
D [cm^2/s]	154 ± 29	108 ± 31	101

Table 9: Derived values and their literature counterpart [VeFP, chap. 6, p.15].

First we have to say, that at both measurements the lowest voltage and the highest distance were not usable. The highest distance gave a m-shaped distribution, while the lowest voltage gave a Gaussian, but one that was way to wide to fit the theoretical implications. Therefore those two were left out from the measurement in most parts.

Some values have relatively high errors. Most of the error propagation comes from our fits. Only the voltage and distance have read-off errors, but ones that are not significant enough

most of the time. Therefore the errors come directly from our measurements and the collected data statistically fluctuating. Since the values are going in two different value directions from the literature values, a systematic shift/error can't be the main reason for the bad results. An error caused by the experimenters is also unlikely, because virtually no data was read-off by hand, and very little things are even adjustable in this experiment.

Both values for the mean lifetime are off significantly from the literature value. It looks like both values are off by a factor of ten. With that factor and the then also ten times larger errors we would be only 2σ off for the constant U measurement and 5σ off for the constant d measurement. Those results would look more like reasonable results. By comparing our results to results from older FP-groups we see that this isn't the first time someone measures this ten times smaller than it should be. Independent experimenters measured the same wrong value over the last decade. Therefore we conclude that the measurement itself probably has a flaw in it, which results in this deviation. Having in mind that the construction of this experiment is a historic one, meaning that it should resemble the original construction and reading the original paper from 1949 [HaySho], where Mr. Haynes and Mr. Shockley measured a mean life span of $10\ \mu\text{s}$ we can safely conclude, that the construction is not suited for an accurate measurement.

Looking at the mobility μ we see that the measurement with a constant distance gave us a more precise and better value than the measure with a constant voltage. For the constant distance we are in a 1σ range of the literature value with a relative error of 3.5%. With the constant voltage we are only in a 5σ range to the literature value, with a relative error of 5.9%. Looking at Figure 13 and 16 we see, that the Gaussian fits for the constant distance look more fitting with what we would expect. In Figure 13 the fits are all over the place in terms of their amplitude and variance. Figure 16 looks more clean and fitting (except of course the tenth fit).

Taking a look at the measured diffusion constants we can see a different picture. The value from the constant distance measurement is very close to the literature value (1σ range). The constant voltage measurement is off quite a bit but still in a 2σ range. That is due to the fact, that the measurement has a relative high relative error of 18.8%. But the constant d measurement has an even bigger relative error of 28.7%. Therefore those measurements aren't really conclusive.

In the third part of the experiment we examined the usability of semiconductors (more precisely a Si-diode and a CdTe-crystal) as detectors. To do so, we measured the radioactive spectra of a ^{241}Am and a ^{57}Co probe, with both detectors. With given energies for the peaks of those probes we then assigned each channel of our MCA to a certain energy. With that we fitted Gaussians to each peak and used them to calculate the absorption probability ratios and the relative energy resolutions of each detector.

The following tables show our results.

peak [keV]	Abs-ratio [%]	Literature [%]
59.5	1.9 ± 0.3	1.40
122.06	1.83 ± 0.07	1.83
136.47	-	2.00

Table 10: Absorption ratios at different energies. [VeFP, chap. 6, p.15]

detector	peak [keV]	RER
Si	59.5	0.318 ± 0.008
	122.06	0.078 ± 0.009
	136.47	-
CdTe	59.5	0.477 ± 0.002
	122.06	0.175 ± 0.004
	136.47	0.139 ± 0.006

Table 11: Relative energy resolution of a CdTe and Si detector.

First of all we didn't measure a second peak at 136.47 keV with the Si detector and the ^{57}Co probe. This is due to the fact, that the probe is a very old one and not that active anymore, because ^{57}Co has a half-life of 270 days and the probe is some years old. We measured for two hours with it, but should have measured five to six hours in order to get better results. Sadly that wasn't possible, because another group needed the same probe for their measurements. Therefore we couldn't calculate the Abs-ratio and the RER for that energy and the Si detector.

As we can see in Table 10 the Abs-ratio for the 59.5 keV peak is within a 2σ interval to the literature value, with a relative error of 15.8%. The Abs-ratio for the 122.06 keV peak matches the literature value with a relative error of 3.8%. We can conclude, that the experiment construction is a good way of measuring the spectra. But it can only give results if we know the energy of the peaks before hand.

With the results from Table 11 we can conclude, that the higher the energy we measure, the more precise our measurement is. Both detectors show that behaviour. The Si and CdTe detectors show a significant increase of resolution when doubling the energy from about 60 to 120 keV.

This overall higher accuracy can also be observed in Table 10, where we receive a better Abs-ratio for the higher energy.

We conclude, that the Si detector has a lower absorption probability than the CdTe which makes it less precise in the eyes of number of events not detected, but it shows a better relative energy resolution than the CdTe crystal. Therefore both detectors have their own sweet spot of usability with high accuracy.

A. List of Figures

1.	Representation of different energy levels/bands at different amounts of electrons and potential wells.	4
2.	indirect (left) and direct semiconductor (right).	5
3.	electron-density n_e and hole-density n_i at a p-n-crossing.	7
4.	Schematic setup, measurement of the band gap.	8
5.	Method of the analysis.	10
6.	Way of the light.	11
7.	Calculation of the wave length for silicon at negative angles.	12
8.	Calculation of the wave length for silicon at positive angles.	12
9.	Calculation of the wave length for germanium at negative angles.	13
10.	Calculation of the wave length for germanium at positive angles.	14
11.	Schematic setup of the Haynes & Shockley-experiment.	15
12.	Data and Gaussian fits for the electron clouds at different laser to needle distances.	16
13.	Exponential fit of the amplitudes of our Gaussian fits.	17
14.	Velocity of the electron clouds with a linear fit.	18
15.	Plot and linear fit for the squared diffusion constant.	19
16.	Exponential fit of the amplitudes of our Gaussian fits.	20
17.	Data and linear fit for the mobility μ_n	21
18.	Plot and linear fit for the squared diffusion constant.	22
19.	Schematic setup of a semiconductor detector.	23
20.	Spectrum from a radioactive ^{241}Am sample using a CdTe-crystal as the detector.	24
21.	Spectrum from a radioactive ^{241}Am sample using a Si-semiconductor as the detector.	24
22.	Spectrum from a radioactive ^{57}Co sample using a CdTe-crystal as the detector.	25
23.	Spectrum from a radioactive ^{57}Co sample using a Si-semiconductor as the detector.	25
24.	Segment from Figure 23.	26
25.	Energy calibration for the Si and CdTe detectors. (The error bars are too small so be visible.)	27
26.	Energy calibrated spectrum of the ^{57}Co probe with the CdTe-detector.	27
27.	Measured data for silicon.	34
28.	Measured data for germanium.	34
29.	Exponential fit of the amplitudes of our Gaussian fits with the original data.	35
30.	Plot and linear fit for the squared diffusion constant with the 10 th data point included.	35
31.	Spectrum from a radioactive ^{241}Am sample using a CdTe-crystal and a Si-semiconductor as the detectors with error bars \sqrt{n}	36
32.	Spectrum from a radioactive ^{57}Co sample using a CdTe-crystal and a Si-semiconductor as the detectors with error bars \sqrt{n}	36

B. List of Tables

1.	errors on amplitudes	9
2.	data of Figure 7	12
3.	data of Figure 8	13
4.	data of Figure 9	13
5.	data of Figure 10	14
6.	Absorption ratios at different energies. [VeFP, chap. 6 ,p.15]	28
7.	Relative energy resolution of a CdTe and Si detector.	28
8.	Data from the literature.	29

9. Derived values and their literature counterpart [VeFP, chap. 6, p.15]. 29
10. Absorption ratios at different energies. [VeFP, chap. 6, p.15] 30
11. Relative energy resolution of a CdTe and Si detector. 31

C. References

- [HaySho] J. R. Haynes and W. Shockley, *Investigation of Hole Injection in Transistor Action*, Phys. Rev., Volume 75, Issue 4, pages 691-691, Year 1949, American Physical Society, <https://link.aps.org/doi/10.1103/PhysRev.75.691>
- [Wal] W. Walcher, *Praktikum der Physik* 1979, B.G. Teubner Stuttgart
- [Sze] S.M. Sze, *Physics of Semiconductor Devices 2nd Edition* 1981, John Wiley Inc.
- [Kit] Ch. Kittel, *Einführung in die Festkörperphysik 7. Auflage* 1988, R. Oldenbourg Verlag München Wien
- [Amr] S. M. Amrein, *Halbleiter & Halbleiterdetektoren*, Staatsexamensarbeit, Physikalisches Institut, Fakultät für Mathematik und Physik, Albert-Ludwigs-Universität Freiburg
- [VeFP] S. Amrein et al., *Versuchsanleitung Fortgeschrittenen Praktikum Halbleiter*, Physikalisches Institut, Fakultät für Mathematik und Physik, Albert-Ludwigs-Universität Freiburg

D. Appendix

D.1. Extra plots

Measurement of the band gap

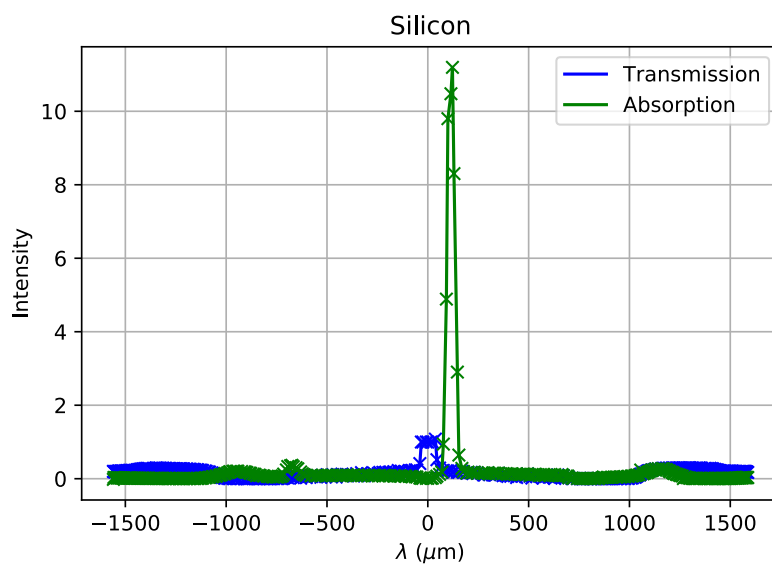


Figure 27: Measured data for silicon.

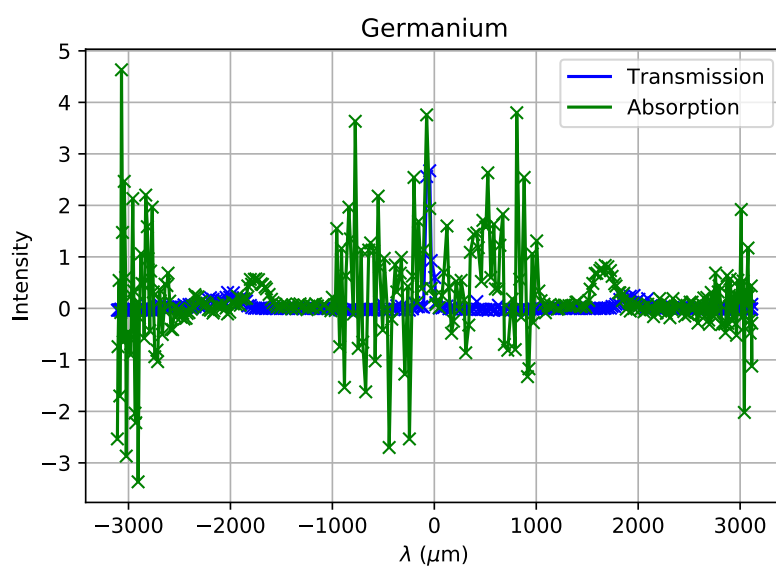


Figure 28: Measured data for germanium.

Haynes & Shockley-experiment

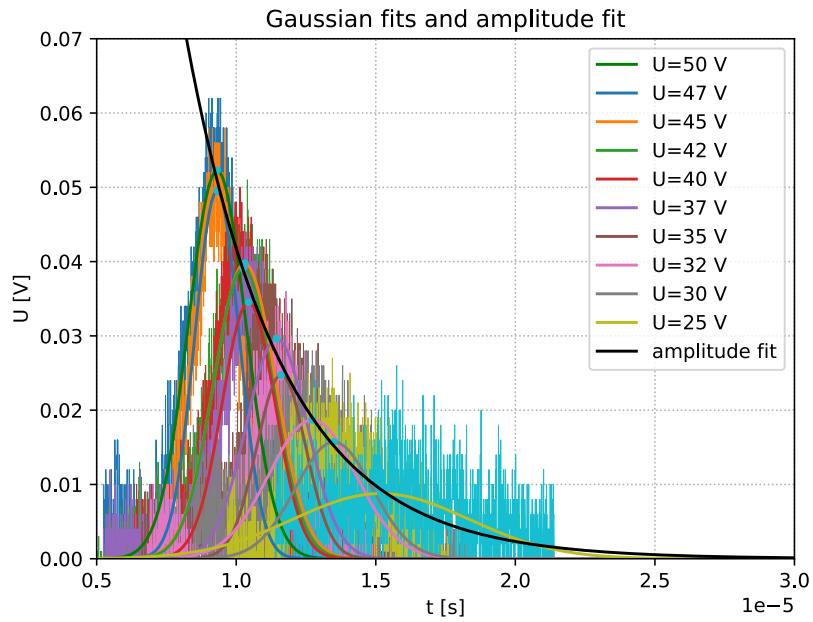
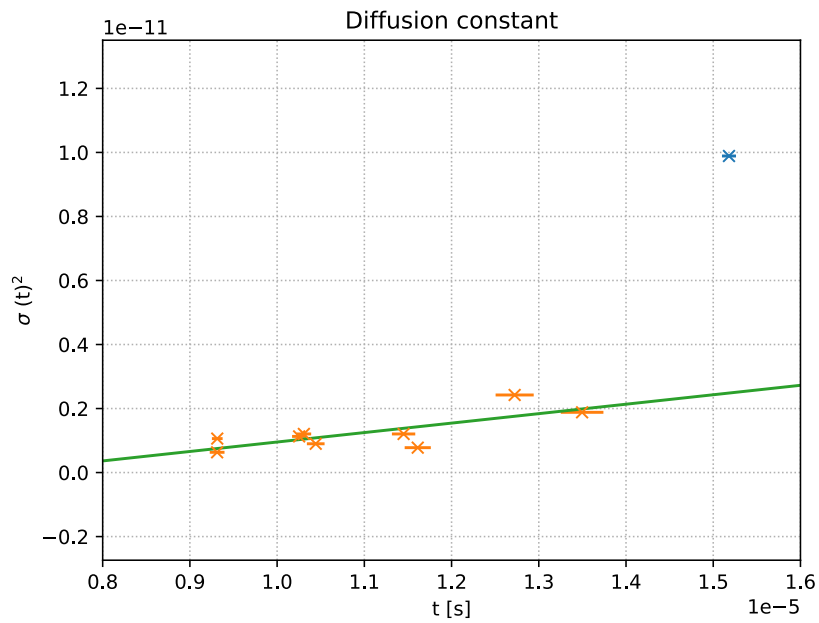


Figure 29: Exponential fit of the amplitudes of our Gaussian fits with the original data.

Figure 30: Plot and linear fit for the squared diffusion constant with the 10th data point included.

Semiconductor detector

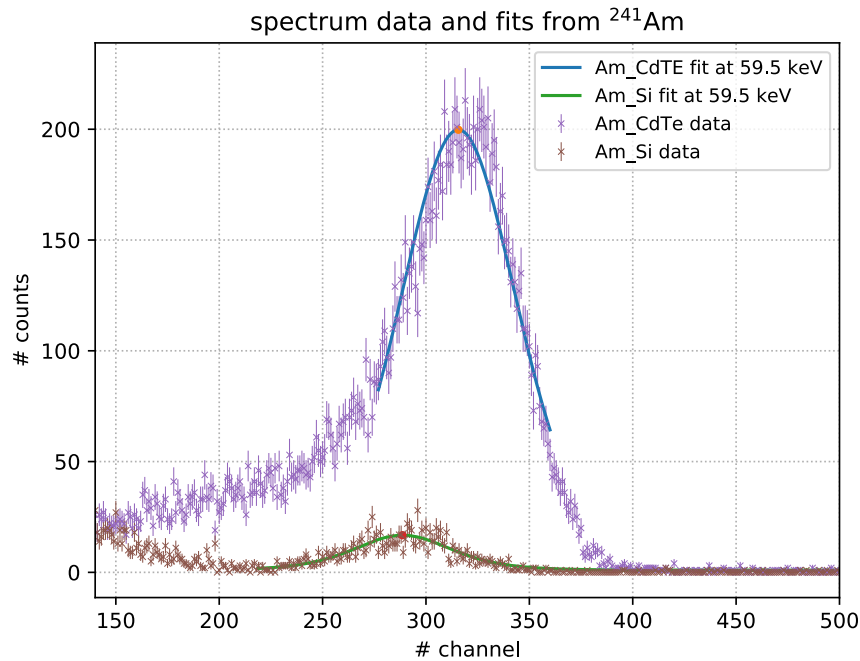


Figure 31: Spectrum from a radioactive ^{241}Am sample using a CdTe-crystal and a Si-semiconductor as the detectors with error bars \sqrt{n} .

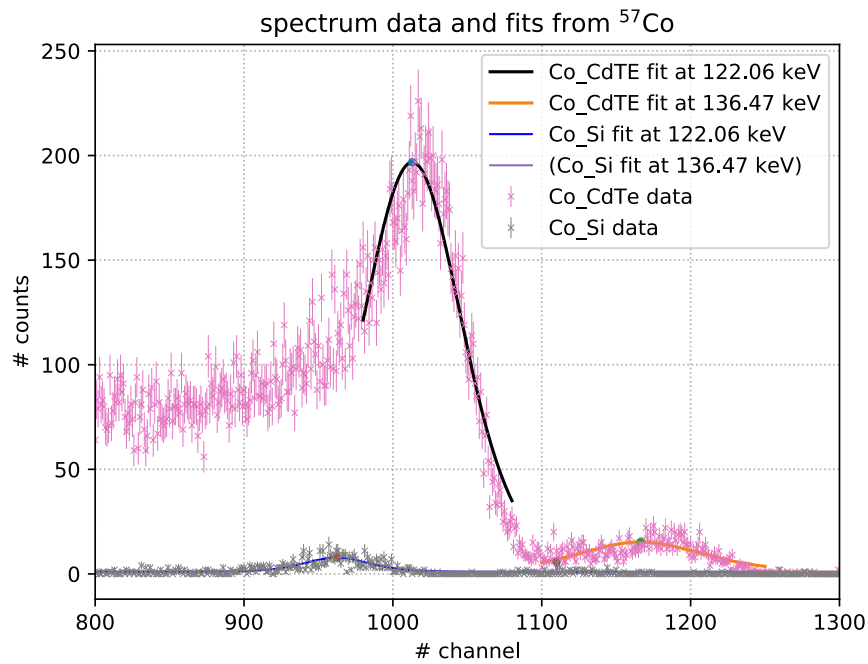


Figure 32: Spectrum from a radioactive ^{57}Co sample using a CdTe-crystal and a Si-semiconductor as the detectors with error bars \sqrt{n} .

D.2. Original data

Blendenweite (2,0³ ~~cm~~ ^{mm} ± 0,01) cm

Abstand Blende-Opt. Gitter (570 ± 10) mm

Störquelle: sample current springt immer wieder mal
• Winkelanzeige schwankt um 0,3° bei Motor stillstand

Fehlermessung Si

Fehlermessung ~~Si~~ Ge

Pyro (V)	Sample (V)
0,029	0,015
0,031	0,015
0,029	0,015
0,029	0,015
0,031	0,015
0,029	0,015
0,029	0,015
0,031	0,015
0,028	0,015
0,029	0,015
0,031	0,015
0,031	0,015
0,029	0,015

Pyro (V)	Sample (V)
0,006	0,105
0,006	0,085
0,007	0,053
0,006	0,066
0,007	0,042
0,006	0,105
0,006	0,137
0,006	0,121
0,006	0,039
0,006	0,112
0,006	0,192
0,006	0,122
0,006	0,109

Haynes & Shockley

Abstand anfang: $(2,1 \pm 0,1)$ mm

Länge Germanium: $(30 \pm 0,1)$ mm

Messreihe 1 in μ cm
Fehler $\pm 0,1$ cm

4,7
2,0
3,0
4,3
6,0
7,0
8,0
3,0
10,0
2,5

Messreihe 2 in V
Fehler: ± 2

50
47
45
42
40
37
35
32
30
25